International Journal of Control and Automation
Vol.7, No.7 (2014), pp. 299-312
http://dx.doi.org/10.14257/ijca.2014.7.7.25

Approach to Study Bearing Thermal Preload Based on the Thermo-Mechanical Information Interaction Net

Teng Hu[1], Guofu Yin[2], Congying Deng[3]

School of Manufacturing and Engineering, Sichuan University
Chengdu 610065, China
[1]hu.t.scu@gmail.com, [2]gfyin@scu.edu.cn, [3]dcyscu@163.com

Abstract

Owing to all the advantages of angular contact ball bearings (ACBB), including little energy consumption and low friction, etc, ACBB becomes the prior options for supportive components of NC machine tool spindle units. Thermal and mechanical behaviors of rigid-preloaded-ACBB are highly coupled, which produces the thermal preload. For investigating the effects of thermal preload on the bearing performances, this paper presents an ACBB thermo-mechanical information interaction net which is constructed on a collaborative computing platform. During the case study process, the thermo-mechanical information interaction net of a NSK ACBB 70BNR10X is realized. Thermal preload of the given ACBB is then predicted and analyzed through the information interaction net. In addition, effects of thermal preload on the ACBB operational stiffness are studied. With the help of temperature inspecting instrument, temperature tests are provided on the bearing thermo-mechanics test platform to validate the interaction net. Great agreements are found between the results predicted by the interaction net and the datum obtained through experimentation. The proposed information interaction net is useful for investigating the behaviors of running-bearing.

Keywords: *Angular contact ball bearing, Information interaction net, Thermal preload, Operational stiffness*

1. Introduction

Angular contact ball bearings (ACBB) are commonly equipped in machine tool spindle unit. To obtain the required stiffness, ACBB is applied external preload. While the machine tool spindle unit is under high-speed working condition, rigid-preloaded ACBB creates thermal preload due to its highly coupled thermal and mechanical characteristics [1]. The thermal preload causes the ACBB preload to vary, and then affects the ACBB thermal and mechanical behaviors. Meanwhile, thermal preload is also subjected to ACBB real-time thermal and mechanical characteristics, as is shown in Figure1.

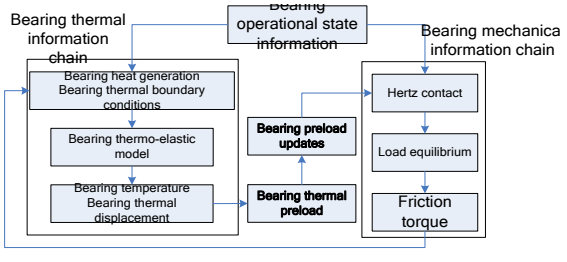

Figure 1. Thermal Preload as a Connection Factor

ISSN: 2005-4297 IJCA

The basis of ACBB mechanical analysis is presented in [2-5], where the quasi-dynamics theory was adopted. Both centrifugal force and gyroscopic moment, which are so-called high-speed effects, were considered in these literatures. De Mul *et al.*, [6] included centrifugal forces in their bearing model, and presented the bearing stiffness in Jacobian matrix form. However, they neglected the gyroscopic moment effect in their formulation. Zverv *et al.*, [7] proposed the principles of selecting the appropriate bearing type for spindle unit after the linear elastic problem of rolling bearings was studied. Kang Y *et al.*, [8] modified the Jones-Harris model to investigate the deep-groove ball bearings based on Hertz contact theory. Moreover, they [9] used neural network to calculate the rolling bearing operational stiffness. Effects of centrifugal force and gyroscopic moment on the ACBB deformation and stiffness were studied by Jedrzejewski *et al.*, [10]. Mechanical characteristics of bearings with different configuration and structural parameters were studied by Guo Y *et al.*, [11]. Cao *et al.*, [12] proposed a method to investigate the effects of different preload mechanism on the nonlinear mechanical behavior of ACBB. It is noteworthy to mention that they employed the Jones' bearing model [4] to evaluate the bearing stiffness in their mathematical model. However, this model did not consider the thermal behavior of ACBB. Ozturk *et al.*, [13] presented one of the most comprehensive mechanical analyses of ACBB. They calculated the dynamic parameters of spindle unit under different bearing preload. Though their work can be applied to predict the cutting stability more accurately but, no thermal effects were considered in the presented methodology.

There have been attempts to model the thermal behavior of ACBB. By the virtue of a complex heat transfer flow diagram, Bossmanns and Tu [14] employed the transient finite difference approach to study the thermal behavior of ball bearing. Jin *et al.*, [15] formulated the theoretical model for ACBB of machine tool ball screw. And the model was verified by experimentation carried on thermal dynamic analysis apparatuses. Discarding the nonlinear mechanical characteristics of ball bearing, Lin *et al.*, [16] proposed an integrated thermo-mechanical-dynamic model to investigate the spindle capabilities. The method they proposed to calculate bearing thermal preload can be easily adapted to a variety of rolling bearings. But the drawback is that they ignore the bearing nonlinear mechanical behavior which is obviously affected by its thermal characteristics. Sun-Min Kim *et al.*, [17] presented a numerical method to establish a comprehensive model for predicting a spindle-bearing system thermo-elastic behavior. Amit *et al.*, [18] employed Parabolic Temperature Profile Approximation to study thermal effects in non-circular journal bearings. Also a comprehensive research for thermal pressure and oil film temperature etc. was carried out. Jin Kyung Choi *et al.*, [19] studied the thermal characteristics of spindle-bearing system by using finite element (FE) method. Based on the proposed FE model, bearing temperature was predicted. A prototype of spindle bearing system was manufactured to verify the numerical model too. Pruvot *et al.*, [20] estimated the temperature of bearing rolling elements by using first-order differential equation. Besides, they presented a model in which both thermal energy balance and complex boundary condition were considered.

Most of the previously developed ACBB models fail to provide a precise analysis result for thermal preload. In order to ensure the reliable operation of ACBB, it is essential and reasonable to calculate the thermal preload precisely so that the comprehensive integrated thermo-mechanical ACBB model can be developed.

In this research, we present a thermo-mechanical information interaction net of ACBB. The interaction net consists of two information chain models: nonlinear mechanical and thermal information chain. The former model allows for all types of ACBB, and the later one

considers comprehensive heat generation laws and exhaustive boundary conditions. An approach to analyze ACBB thermal preload is proposed. During the case study process, thermo-mechanical information interaction net of a NSK ACBB 70BNR10X is constructed. Thermal preload datum are then calculated and studied with respect to different rotational velocities. Effect of thermal preload on ACBB operational stiffness is investigated as well. The interaction net is validated through temperature tests by the virtue of temperature inspecting instrument.

This paper is organized as follows: ACBB nonlinear mechanical information chain model is established mathematically in Section2. Section3 is mainly focused on formulating the thermal information chain model of ACBB. In Section4, ACBB thermo-mechanical interaction net is realized on a collaborative computing platform of ANSYS and MATLAB. In Section5, we establish NSK 70BNR10X ACBB thermo-mechanical information interaction net, based on which thermal preload is calculated and analyzed, too. Experimental verification is discussed in Section6. Finally the conclusions are laid out in Section 7.

2. ACBB nonlinear Mechanical Information Chain Model

2.1. Topology Diagram of ACBB Nonlinear Mechanical Information Chain Model

Due to the effects of centrifugal force and gyroscopic moment, speed-varying mechanical behaviors of ACBB must be considered. In order to establish the ACBB nonlinear mechanical information chain model, we propose the following concepts:

①Eigen information. It concerns ACBB geometry and material, which are related to the bearing producer. It has nothing to do with the working condition. ②Operational state information. It includes initial preload, rotational velocity *etc.*, ③Performance information. It consists of friction torque, contact load and contact stiffness, *etc*. Thus the topological diagram of ACBB nonlinear mechanical information chain model is shown in Figure 2.

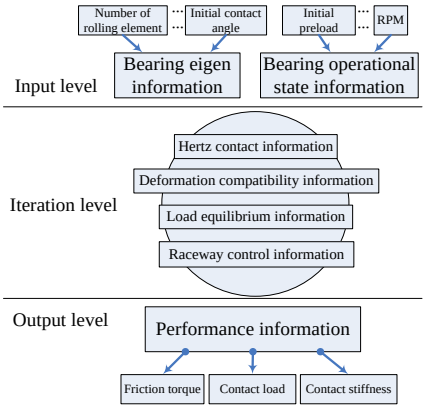

Figure 2. Nonlinear Mechanical Information Chain Model of ACBB

2.2. The Hertz contact of ACBB

Assume that Q_{ij} and Q_{ej} are contact loads between the jth ball and rings, where the subscript i and e represent the inner ring and outer ring, respectively. Thus according to the Hertz contact theory, Q_{ij} and Q_{ej} can be evaluated as Equation (1). On the basis of

the definition of contact stiffness, we can express the contact stiffness between the *j*th ball and rings K_{ij}^{B} and K_{ej}^{B} as Equation (2)

$$Q_{ij} = k_{ij}\delta_{ij}^{1.5} \quad Q_{ej} = k_{ej}\delta_{ej}^{1.5} \quad (1)$$

$$K_{ij}^{B} = 1.5k_{ij}\delta_{ij}^{0.5} \quad K_{ej}^{B} = 1.5k_{ej}\delta_{ej}^{0.5} \quad (2)$$

where k_{ij} and k_{ej} are the Hertz contact coefficients, δ_{ij} and δ_{ej} are the contact deformation due to the external load.

2.3. Acquisition of the ACBB Performance Information

According to the azimuth diagram shown in Figure3(a), the global bearing force equilibrium function can be established. The bearing internal deflection compatibility and the load equilibrium relationship of individual rolling element can be derived based on the relationship in Figure3(b) and Figure3(c). Later the ACBB performance information, including the operational stiffness, contact load and friction torque, can be evaluated by Newton-Raphson method iteratively. The calculation procedure is depicted in Figure4.

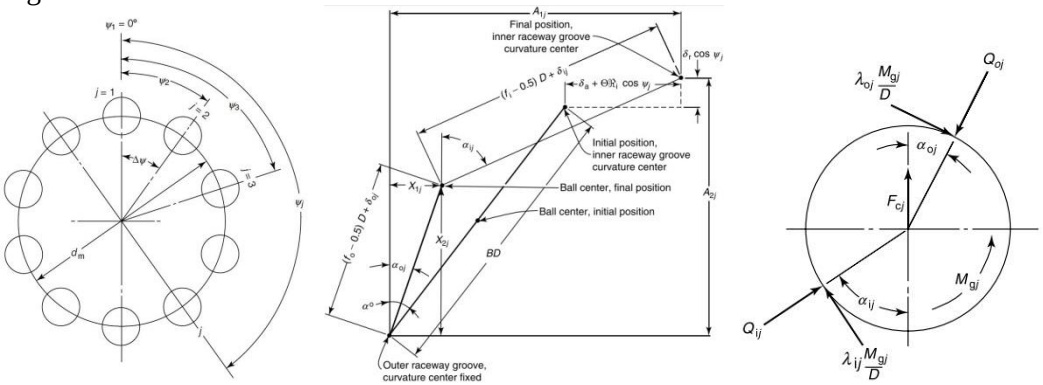

Figure 3. (a) Azimuth of ACBB, (b) Deformation Relationship Between ball and Rings, (c) Mechanics Analysis of Ball

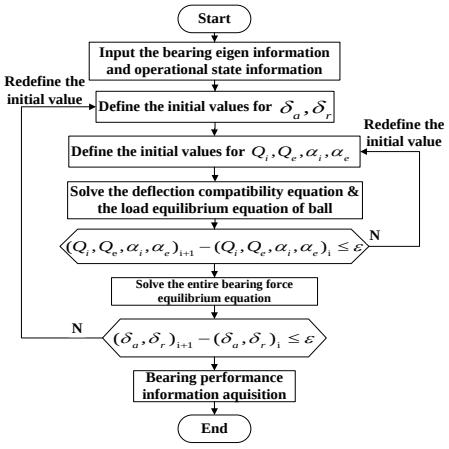

Figure 4. Acquisition Procedure of ACBB Performance

3. ACBB Thermal Information Chain Model

3.1. Topology Diagram of ACBB Thermal Information Chain Model

Basically, ACBB heat generation caused by friction can be categorized in three groups: load-related, lubrication-viscosity-related and ball-spin-motion-related. Furthermore, ACBB heat transfer process is mainly affected by the bearing thermal boundary condition. Therefore, for the purpose of correctly understanding the topological diagram of ACBB thermal information chain model presented in Figure5, following concepts should be paid attention:

①Friction is the measurement of ACBB energy loss, namely heat generation. In order to predigest the analysis, we assume that 50% of the total heat generation is allocated to rolling elements, and that the left 50% is averagely allocated to inner and outer ring. ② Conduction and convection are the mainly expected heat transfer approaches of ACBB. Radiation is simply ignored. ③The inner core of the thermal information chain proposed in this Section is ACBB thermo-elastic model. ACBB temperature and thermal displacement are calculated through the thermo-elastic model.

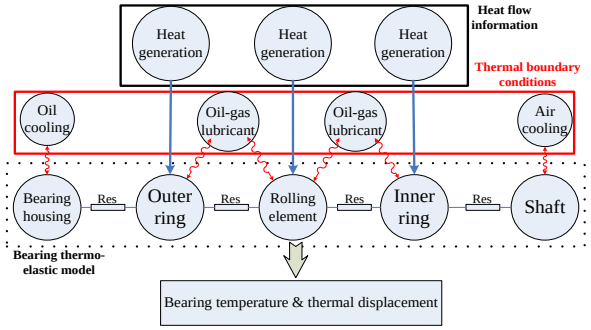

Figure5. Thermal Information Chain Model of ACBB

3.2. ACBB Heat Generation

According to the contents in 3.1, the total ACBB friction torques can be expressed:

$$M_{total} = M_l + M_v + M_s \qquad (3)$$

where $\boldsymbol{M}_l$ is the load-related friction torque, $\boldsymbol{M}_v$ is the lubrication-viscosity-related friction torque, and $\boldsymbol{M}_s$ is the ball-spin-motion-related friction torque. Hence, ACBB heat generation is given as:

$$Q = \frac{2\pi}{60} n\left(M_l + M_v\right) + \sum_{j=1}^{Z} M_{sj}\omega_{sj} \qquad (4)$$

where n represents the rotational velocity, $\omega_{sj}$is the spin speed of the jth ball, and Z is the number of rolling elements.

3.3. ACBB Thermal Boundary Condition

3.3.1. Thermal Contact Resistance between Balls and Rings

Thermal contact resistance between balls and rings is subjected to the Hertz contact area which can be obtained through the ACBB nonlinear mechanical information chain model. Then the thermal resistance R is [21]:

$$R = \frac{\psi}{4\lambda_1 a} + \frac{\psi}{4\lambda_2 a} \qquad (5)$$

where $\psi = \frac{2}{\pi}\int_0^{\pi/2} \frac{d\theta}{\sqrt{\left(1 - k^2 \sin^2 \theta\right)}}$, and $k = 1 - \frac{b^2}{a^2}$. a, b are the Hertz contact ellipse semi-axis and ellipse minor axis, respectively. $\boldsymbol{\psi}$ is the geometry factor which is related to the Hertz contact area. $\boldsymbol{\lambda_1}$ and$\boldsymbol{\lambda_2}$ are the thermal conductivity coefficients of rolling elements and rings, respectively.

3.3.2. Conduction Coefficients of Joints between Outer Ring and Bearing Housing

Generally, clearance, which is temperature dependent, exists in the joints between outer ring and bearing housing. Thus, if the thermal expansion coefficient of bearing housing $\boldsymbol{\alpha}$ is known, conduction coefficients of joints follow the relationship proposed by Bossmanns [14]:

$$h_c = \frac{1}{h_{ring} \Big/ \lambda_{ring} + h_{gap} \Big/ \lambda_{air}} \cdot A \qquad (7)$$

$$h_{gap} = h_{gap\,0} - \left(T_{ring} - T_{housing}\right)\alpha \cdot r_{housing} \qquad (8)$$

where $\boldsymbol{\lambda_{ring}}$, $\boldsymbol{\lambda_{air}}$ are the thermal conductivity coefficients of outer ring and air, respectively. A is the outer surface area of outer ring. h_{ring} is known as the thickness of outer ring. h_{gap} and h_{gap0} represent the average clearance thickness and its initial value, respectively. T_{ring}, $T_{housing}$ are the temperatures of outer ring and bearing housing, respectively. And $r_{housing}$ denotes the radius of bearing housing.

3.3.3. Thermal Contact Resistance between Inner Ring and Shaft

If the inner ring conduction coefficient $\boldsymbol{\lambda_1}$ and the shaft conduction coefficient $\boldsymbol{\lambda_2}$ are known, thermal contact resistance between inner ring and shaft R can be expressed as Equation (9) based on the fractal model described in [22]:

$$R = 1 \Big/ Ah_c \qquad (9)$$

$$h_c = \frac{1}{L_g} \cdot A_r^* \cdot \frac{2\lambda_1\lambda_2}{\lambda_1 + \lambda_2} \qquad (10)$$

where $\boldsymbol{A}_r^*$ and A are the dimensionless real contact area and nominal contact area, respectively. L_g is the clearance thickness of joint.

3.3.4. Convection Coefficients of ACBB

Computing methods of ACBB convection coefficients are shown in Table 1, where the Nusselt number, *Nu*, is obtained from Reynolds number *Re* and Prandtl number *Pr* with respect to different thermal boundary condition.

Table 1 Thermal Boundary Information of ACBB

Thermal boundary condition	Convection coefficients	Nusselt number
Bearing housing cooling liquid convection	$\alpha_c = Nu\,\lambda / D$	$Nu = 1.86\,(Re \cdot Pr \cdot \frac{D}{L})^{1/3}$
Oil-gas lubricant convection		$Nu = 0.023 \cdot Re^{0.8} \cdot Pr^{0.3}$
Rotating component end face convection	$\alpha_c = 28\,(1 + \sqrt{0.45 \cdot \bar{u}})$	
Rotating component outer surface convection	$\alpha_c = c_0 + c_1 \cdot \bar{u}^{c_2}$	
Non-rotating component surface convection	$\alpha_c = 9.7$	

3.4 ACBB Thermo-elastic Model

Based on the laws of thermodynamics [23]-[24] and the theory of finite element method [25], ACBB thermo-elastic model would be:

$$\begin{bmatrix} [M] & [0] \\ [0] & [0] \end{bmatrix} \begin{Bmatrix} \{\ddot{u}\} \\ \{\ddot{T}\} \end{Bmatrix} + \begin{bmatrix} [C] & [0] \\ [C^{tu}] & [C^{t}] \end{bmatrix} \begin{Bmatrix} \{\dot{u}\} \\ \{\dot{T}\} \end{Bmatrix} + \begin{bmatrix} [K] & [K^{ut}] \\ [0] & [K^{t}] \end{bmatrix} \begin{Bmatrix} \{u\} \\ \{T\} \end{Bmatrix} = \begin{Bmatrix} \{F\} \\ \{Q\} \end{Bmatrix} \quad (11)$$

$[M]$, $[K]$, and $[C]$ are the ACBB mass, stiffness and damping matrices, respectively. $[C^{tu}]$ represents the thermo-elastic damping matrix. $[C^t]$ is the specific heat matrix. $[K^{ut}]$ is the thermo-elastic stiffness matrix. $[K^t]$ is the heat transfer matrix, which is the combination of conductivity matrix and convection matrix. $\{F\}$ and $\{Q\}$ are the force vector and thermal load vector, respectively. $\{u\}$ and $\{T\}$ are displacement vector and temperature vector, respectively. The strongly coupled nonlinear Equation (11) can be solved by Newmark method [25]. Thus the ACBB temperature and thermal displacement are derived.

4. ACBB thermo-mechanical Information Interaction Net

ACBB thermo-mechanical information interaction net is established on a collaborative computing platform that combines ANSYS and MATLAB software. Frame of the proposed interaction net is illustrated in Figure 6.

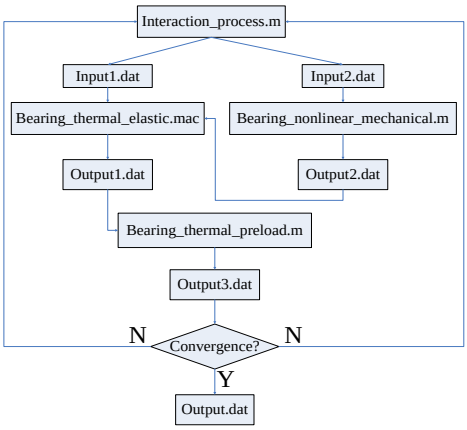

Figure 6. Frame of ACBB Thermo-mechanical Information Interaction Net

Using the theory given in Section2, ACBB nonlinear mechanical information chain model (Bearing_nonlinear_mechanical.m) is developed in MATLAB environment. In according with the contents described in Section3, angular contact ball bearing thermal information chain model (Bearing_thermal_elastic.mac) is created in ANSYS environment with the help of ANSYS Parametric Design Language. Thermal preload P_{th} computing method presented here (Bearing_thermal_preload.m) is similar to Lin's [16]:

$$\varepsilon_t = \varepsilon_b + \varepsilon_r \cos \alpha - \varepsilon_a \sin \alpha \quad (12)$$

$$P_{th} = k_t \varepsilon_t^{\,n} \quad (13)$$

where $\varepsilon$is the thermal displacement, subscript *t*, *b*, *r*, and *a* represent total, balls, radial direction of rings and axial direction of rings, respectively. k_t is the coefficient for elastic contact.

However, we modify Lin's method to make it become an iterative process. As is illustrated in Section1, thermal preload, connecting the two information chain models above, is the interactive consequence of thermal and mechanical behaviors of ACBB. Therefore, a governing program (Interaction_process.m) for coupling the two models above is written in MATLAB. Bearing displacement, temperature and thermal preload are updated at each iteration step.

To ensure the convergence, we set $\Delta_1=10^{-1}$, and$\Delta_2=1$, whereΔ_1 is the convergence criterion for displacement and temperature, Δ_2 is the convergence criterion for thermal preload.Once the convergence criterion is achieved, ACBB thermo-mechanical information interaction process reaches a dynamic equilibrium condition. As of this moment, bearing heat dissipation rate is even with the rate of heat generation. ACBB temperature changes no more, and thermal preload stabilizes. The entire results, namely ACBB temperature, thermal preload and operational stiffness, etc. are written in output file (Output.dat).

5. Example and Results Analysis Thermal Preload

5.1. Thermal Preload Calculation

To validate the ACBB thermo-mechanical information interaction net defined in Section 4, NSK 70BNR10X ACBB used for high-speed spindle unit is investigated. Assume that the given bearing is rigid preloaded and that the initial preload is selected

as 285N (Extreme Light, EL) [26]. The maximum bearing rotational velocity is 20000rpm. Lubrication mechanism is designed to be oil-gas, kinematic viscosity of which is 22cst at the temperature of 40℃. Compressed air flow speed is 2.5×10^{-3}/s. Some other eigen information is manifested in Table 2.

Table 2. 70BNR10X Eigen Information

Inner radius	Outer radius	Ring thickness	Ball diameter	Initial contact angle	Mass	Number of balls
70mm	110mm	20mm	8.731mm	18°	0.605kg	25

Information interaction net is then programmed. Thermal preloads (shown in Figure 7) are obtained when program stops running for the criterion of convergence is achieved. It is easily indicated that ACBB thermal preload is proportional to rotating velocity. Figure 7 also shows the variation that thermal preload increases at first, decreases later, and finally stabilizes. Explanation is given as follow:

Firstly, it can be observed from Equation (12) that thermal displacements of rolling element and that of rings in radial direction have a positive contribution to ACBB thermal preload. Contrarily, thermal displacement of rings in the axial direction minifies the thermal preload. Secondly, as components of ACBB have distinguishing thermal boundary conditions (Figure 5), inner and outer ring thermal displacements variations are different. In detail, in the initial phase of bearing working state, rolling element is the major heat generation source. Due to the light weight of rolling element compared to rings, temperature of rolling element is much greater than that of rings. As time passes by, a portion of heat transfers to rings, and dissipates through the bearing housing and shaft. Thus the temperature difference between rolling element and rings is becoming smaller. Finally, when ACBB reaches the thermal equilibrium, thermal preload stabilizes.

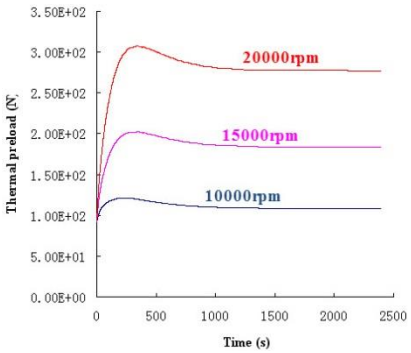

Figure 7. Thermal Preload vs. Velocity

5.2. Effects of Thermal Preload on ACBB Operational Stiffness

Predicted by the interaction net, stable thermal preloads of 70BNR10X ACBB running at the speeds of 10000rpm, 15000rpm and 20000rpm are 109N, 184N and 277N, respectively. Operational stiffness at the same speeds is extracted from the ACBB thermo-mechanical information interaction net (shown in Figure 8).

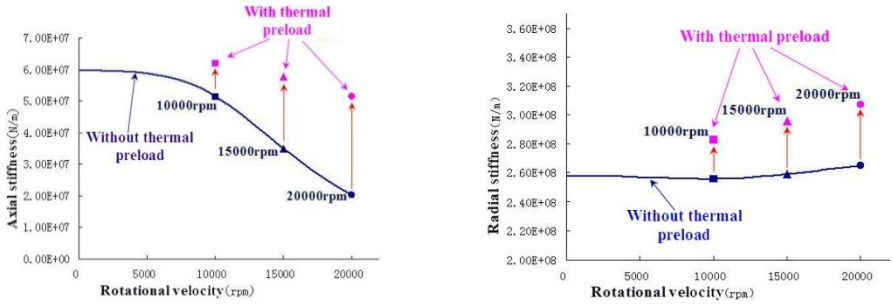

(a) axial operational stiffness (b) radial operational stiffness

Figure 8. Effect of Thermal Preload on Bearing Operational Stiffness

It can be seen that ACBB thermal preload enhances the operational stiffness considerably, where the stiffness augment amplitude is proportional to the rotational velocity. The increased bearing stiffness can raise spindle unit natural frequency, which can ensure that the spindle unit working speed range shall avoid the critical speed. Nevertheless, the risk exists that bearing temperature will rise rapidly, and most likely until the lubricant deteriorates, ultimately causing bearing failure.

6. Experimental Validation

Bearing thermo-mechanical experimental platform shown in Figure 9 is built based on a high-speed spindle unit which is fixed on a test bed. Four NSK 70BNR10X ACBBs mounted in the spindle unit are rigid preloaded with Double Back to Back (DBB) arrangement.

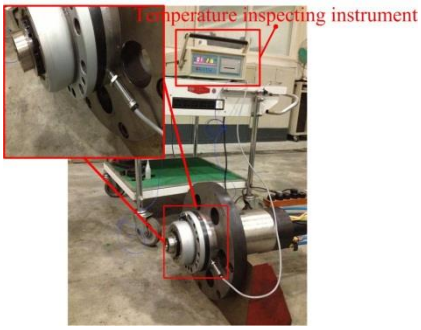

Figure 9. ACBB Experimentation Setup

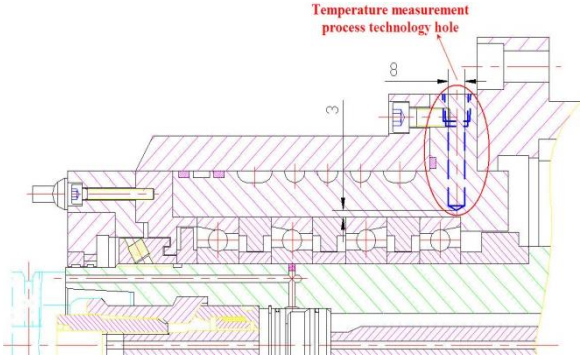

Figure 10. The Temperature Measurement Hole

Temperature tests are carried out with respect to three different rotational velocities: 10000rpm, 15000rpm and 20000rpm at the constant ambient temperature of 15℃. Temperature inspecting instrument is employed to measure the temperature of bearing outer ring through a process technology hole manufactured (shown in Figure10). Figure11 shows that agreement between the results derived from ACBB thermo-mechanical information interaction net (solid line) and the datum obtained from temperature tests (dots) is excellent.

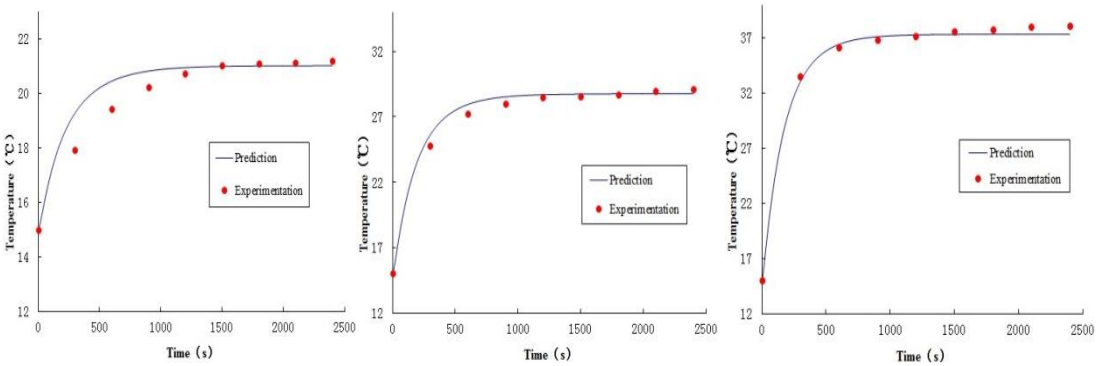

(a) 10000rpm (b) 15000rpm (c) 20000rpm

Figure 11. Bearing Outer Ring Temperature vs. Velocity

7. Conclusions

Considering the nonlinear mechanical behaviors and the exhaustive thermal boundary conditions, an ACBB thermo-mechanical information interaction net is developed to study the thermal preload comprehensively. The presented interaction net is validated experimentally through temperature tests. Based on the results derived from interaction net and experimentation, we can draw the conclusions as follow:

①Mechanical characteristics of ACBB are not time-independent due to thermal preload which is the interaction result of highly coupled ACBB mechanical and thermal behaviors.

②Nonlinear variation of ACBB thermal preload is caused by the different thermal boundary conditions of rolling elements and rings.

③Thermal preload can enhance the ACBB operational stiffness considerably.

④Although the increased ACBB operational stiffness can raise the spindle unit natural frequencies, which ensures that spindle working speed range would avoid the critical speed, it also may result the bearing failure due to the extremely rapid temperature rise.

Acknowledgements

The authors were supported by the National Science and Technology Major Projects Grant 2013ZX04005-012.

References

[1] J. Mayr, J. Jedrzejewski, E. Uhlmann, M. A. Donmez, W. Knapp, F. Hartig and K. Wendt, Toshimichi Moriwaki, Paul Shore, Robert Schmitt, Christian Brecher, Timo Wurz, Konrad, Wegener, "Thermal issues in machine tools", CIRP Annals Manufacturing Technology, no. 2, **(2012)**, pp. 1-21.
[2] A. H. Tedric and N. K. Michael, "Rolling bearing analysis", 3rd. John Wiley & Sons, Inc. **(1990)**.
[3] P. Arvid, "Ball and roller bearing engineering", 3rd ed. Philadelphia: Burbank, **(1959)**.
[4] A. B. Jones, "Ball motion and sliding friction in ball bearings", Journal of Basic Engineering, no. 3, **(1959)**, pp. 1-15.
[5] A. B. Jones, "A general theory for elastically constrained ball and radial roller bearings under arbitrary load and speed condition", Journal of Basic Engineering, vol. 2, **(1960)**, pp. 309-320.
[6] J. M. De Mul, J. M. Vree and D. A. Maas, "Equilibrium and Associated Load Distribution in Ball and Roller Bearings Loaded in Five Degrees of Freedom While Neglecting Friction—Part I: General Theory and Application to Ball Bearings", Journal of Tribology, vol. 111, no. 1, **(1989)**, pp. 142-148.
[7] I. Zverv, Y. S. Pyoun, K. B. Lee, J.-D. Kim, I. Jo and A. Combs, "An elastic deformation model of high speed spindles built into ball bearings", Journal of Materials Processing Technology, vol. 170, **(2005)**, pp. 570–578.
[8] Y. Kang, P. C. Shen, C. C. Huang, S.-S. Shyr and Y.-P. Chang, "A modification of the Jones–Harris method for deep-groove ball bearings", Tribology International, vol. 39, **(2006)**, pp. 1413–1420.
[9] Y. Kang, C. C. Huang, C. S. Lin, P.-C. Shen and Y.-P. Chang, "Stiffness determination of angular-contact ball bearings by using neural network", Tribology International, vol. 39, **(2006)**, pp. 461–469.
[10] J. Jedrzejewski and W. Kwasny, "Modelling of angular contact ball bearings and axial displacements for high-speed spindles", CIRP Annals - Manufacturing Technology, vol. 59, **(2010)**, pp. 377–382.
[11] Y. Guo and R. G. Parker, "Stiffness matrix calculation of rolling element bearings using a finite element/contact mechanics model", Mechanism and Machine Theory, vol. 51, **(2012)**, pp. 32–45.
[12] H. Cao, T. Holkup and Y. Altintas, "A comparative study on the dynamics of high speed spindles with respect to different preload mechanisms", International Journal of Advanced Manufacturing Technology, vol. 57, **(2011)**, pp. 871–883.
[13] E. Ozturk, U. Kumar, S. Turner and T. Schmitz, "Investigation of spindle bearing preload on dynamics and stability limit in milling", CIRP Annals Manufacturing Technology, vol. 61, **(2012)**, pp. 343–346.
[14] B. Bossmanns and J. F. Tu, "A thermal model for high speed motorized spindles", International Journal of Machine Tools & Manufacture, vol. 39, **(1999)**, pp. 1345–1366.
[15] C. Jin, B. Wu and Y. Hu, "Heat Generation modeling of ball bearing based on internal load distribution", Tribology International, vol. 45, no. 1, **(2012)**, pp. 8-15.
[16] C. W. Lin, J. F. Tu and J. Kamman, "An integrated thermo-mechanical-dynamic model to characterize motorized machine tool spindles during very high speed rotation", International Journal of Machine Tools & Manufacture, vol. 43, **(2003)**, pp. 1035–1050.
[17] S.-M. Kim and S.-K. Lee, "Prediction of thermo-elastic behavior in a spindle–bearing system considering bearing surroundings", International Journal of Machine Tools & Manufacture, vol. 41, **(2001)**, pp. 809–831.
[18] A. Chauhan, R. Sehgal and R. K. Sharma, "Investigations on the thermal effects in non-circular journal bearings", Tribology International, vol. 44, **(2011)**, pp. 1765–1773.
[19] J. K. Choi and D. G. Lee, "Thermal characteristics of the spindle bearing system with a gear located on the bearing span", International Journal of Machine Tools & Manufacture, vol. 38, **(1998)**, pp. 1017–1030.
[20] F.C. Pruvot, A. Mottu. High Speed Bearings for Machine Tool Spindles, CIRP Annals - Manufacturing Technology, vol. 29, **(1980)**, pp. 293–297.
[21] K. Nakajima, "Thermal contact resistance between balls and rings of a bearing under axial, radial and combined loads", Journal of Thermophysics and Hear Transfer, vol. 9, **(1995)**, pp. 88-95.
[22] M. Xu and S. Jiang, "An improved thermal model for machine tool bearings", International Journal of Machine Tools & Manufacture, vol. 47, **(2007)**, pp. 53-62.
[23] H. Parkus, "Thermoelasticity", Springer-Verlag, **(1976)**.
[24] T. L. Bergman, A. S Lavine, F. P. Incropera and D. P. Dewitt, "Fundamentals of Heat and Mass Transfer", John wiley & Sons, New York, **(2011)**.
[25] R. D. Cook, D. D. Malkus and M. E. Plesha, "Concepts and Applications of Finite Element Analysis", John Wiley & Sons, New York. **(1988)**.
[26] NSK Super precision bearings. CAT.No.E1254f 2011 D-2 Printed in Japan © NSK. Ltd., **(2003)**.

Authors

Teng Hu, he received his M.Sc. in Material Science & Engineering (2011) and now he is a PhD student in School of Manufacture Science & Engineering, Sichuan University. His research interests are CAE & Optimization of the coupling performance of machine tool functional components.

Guofu Yin, was born in Sichuan (China), 1956. He is now a Professor in School of Manufacturing Science and Engineering of Sichuan University (China). His research interests concern: precision and high speed machine tool performances

Congying Deng, was born in Sichuan (China), 1991. She is now a PhD candidate in School of Manufacturing Science and Engineering of Sichuan University (China). Her research interests concern: machine tool dynamics.